Sensitivity of blocks and cyclones in ERA5 to spatial resolution and definition

M. Rohrer[1,2,*], O. Martius[1,2,3], C. C. Raible[1,4], S. Brönnimann[1,2]

[1] Oeschger Centre for Climate Change Research, University of Bern, Bern, Switzerland

[2] Institute of Geography, University of Bern, Bern, Switzerland

[3] Mobiliar Lab for Natural Risks, University of Bern, Bern, Switzerland

[4] Climate and Environmental Physics, Physics Institute, University of Bern, Bern, Switzerland

* Now at: Axis Capital, Zurich, Switzerland

Corresponding author: Marco Rohrer (marco.rohrer@protonmail.ch)

Key Points:

- Characteristics of blocks and cyclones are generally similar in ERA5 and ERA-interim.
- Characteristics are more sensitive to the spatial resolution than the choice of the reanalysis, especially for cyclones.
- We recommend comparing climate model and reanalysis data using a common resolution.

Abstract

ERA5, the fifth-generation reanalysis of the European Center for Medium-Range Weather Forecasts, provides long time series of atmospheric fields at high spatial and temporal resolution. It allows detailed studies of atmospheric flow features such as blocks or cyclones. We investigate characteristics of blocks and cyclones in ERA5 using different algorithms, compare the results to ERA5's predecessor, ERA-interim, and investigate how these characteristics depend on spatial resolution. Generally, ERA5 and ERA-interim characterize blocks and cyclones similarly. For Lagrangian detection and tracking methods, blocks are more robust than cyclones to changes in resolution and reanalysis choice. Eulerian methods are robust to changes in resolution. Thus, ERA5 provides a state-of-the-art reanalysis for the synoptic-scale extra-tropical circulation. We find that Lagrangian cyclone characteristics are strongly dependent on spatial resolution and therefore recommend that model and reanalysis data should be mapped to a common resolution for verification.

Plain Language Summary

Reanalyses are among the most widely used data sets in the geosciences as they provide a state of the atmosphere that is complete in both space and time by combining a

This article has been accepted for publication and undergone full peer review but has not been through the copyediting, typesetting, pagination and proofreading process which may lead to differences between this version and the Version of Record. Please cite this article as doi: 10.1029/2019GL085582

state-of-the-art weather prediction model with historical observations. Their applications range from climatological studies to the closer examination of extreme events. Reanalyses are often the primary tool to assess the performance of climate models. Recently, the ERA5 reanalysis was published and thus many users may consider using this new product. However, due to its novelty, ERA5 is not yet investigated extensively. We examine mid-latitudinal atmospheric flow features such as blocks and cyclones and their dependence on input resolution and choice of reanalysis. We find that blocks and cyclones characteristics are very similar in ERA5 and its predecessor ERA-interim. Input resolution often plays a more important role on block and cyclone characteristics than the choice between ERA5 and ERA-interim, particularly in case of cyclone characteristics. For many applications the full resolution of ERA5 may not be necessary, easing the computational requirement to use this high resolution dataset. In case of modeling studies where reanalysis data is compared to modeled data, we recommend using the same resolution.

Index terms and key words

AGU index set: 1610 Atmosphere, 3309 Climatology, 3364 synoptic-scale meteorology

6 own keywords: Block, cyclone, reanalysis, resolution, ERA5, ERA-interim

1 Introduction

Atmospheric blocks and extratropical cyclones are central features of synoptic-scale variability in the mid-latitudes. Blocks are defined as quasi-stationary, persistent anticyclones that divert the storm track (e.g., Woollings et al., 2018). Cyclones can be defined in various ways, e.g. by a local minimum of sea level pressure or a local maximum in vorticity (e.g., Raible et al., 2008; Neu et al., 2013). They form and move frequently within preferred regions referred to as storm tracks (Shaw et al., 2016). Both blocks and cyclones are linked to extreme weather and climate. Blocks are linked to heat waves (Black et al., 2004), cold spells (e.g., Buehler et al., 2011), and heavy precipitation (e.g., Lau & Kim, 2012; Martius et al., 2013; Lenggenhager & Martius, 2019). Cyclones can lead to heavy precipitation (e.g., Pfahl & Wernli, 2012; Messmer et al. 2015) and strong winds (e.g., Catto, 2016).

Several detection and tracking methods for blocks and cyclones exist (Woollings et al., 2018; Neu et al., 2013; Catto, 2016). Blocks may be identified as regions with a meridional reversal of the geopotential height (Tibaldi & Molteni, 1990; Scherrer et al., 2006), regions with anomalously high geopotential height (Dole & Gordon, 1983; Buehler et al., 2011), or regions with low potential vorticity (PV; Schwierz et al, 2004). Lagrangian methods detect and track blocks and cyclones in space and time (Raible et al., 2008; Neu et al., 2013). In contrast, Eulerian methods examine properties at a given point as a function of time. Storm tracks, regions with highest cyclonic activity, are often defined identified based on a 2.5-6 day band-pass filtered 500 hPa geopotential height (Z500) field, while blocks can be identified by applying a 10 day low-pass filter to the Z500 field (Blackmon, 1976).

Apart from the definition and method, results also depend on the underlying data set and its spatial and temporal resolution (e.g. Blender and Schubert, 2000; Wang et al., 2016; Rohrer et al., 2018). The new ERA-5 data set (Hersbach & Dee, 2016) is available at the unprecedented resolution of approximately 31 km. The data volume at the full resolution and for the entire time period covered by ERA-5 may exceed the storage capacity of potential users and the question arises if data at the full resolution are needed to answer specific research questions. Here, we answer this question for blocking and cyclone by i) exploring the sensitivity of several objective detection algorithms to resolution and by ii) discussing

reasons for the sensitivity. Additionally, the results of this study will enable the reader to assess the validity of former findings of blockings and cyclones based on coarse resolutions.

2 Data and Methods

We use ERA5 and ERA-interim data from 1979 to 2017 at six-hourly resolution. Compared to ERA-interim, ERA5 ingests more data sources, uses an updated numerical weather prediction model and data assimilation system, and provides higher spatial resolution: T639 and 137 horizontal levels compared to T255 and 60 levels for ERA-interim. We only use the deterministic run of ERA5. We bi-linearly remap the data to a resolution of 1° and 2° for the blocking identification. For cyclones, we remap to the T63 resolution by spectrally truncating at wave number 63 instead of the 2° resolution as some cyclone detection and tracking methods apply spectral remapping to the input data (e.g., Hodges, 1995).

We employ three Lagrangian blocking algorithms that are variations of the blocking algorithm used by Rohrer et al. (2018):

1) TM2D: A 2-dimensional extension of the Tibaldi & Molteni (1990) blocking definition (Scherrer et al., 2006). The following two criteria must be fulfilled to detect a block:

i) Z500 gradient towards pole: $$Z500G_P = \frac{Z500_{\varphi+d\varphi} - Z500_{\varphi}}{d\varphi} < -10 \ \frac{m}{^\circ lat} \quad (1)$$

ii) Z500 gradient towards equator: $$Z500G_E = \frac{Z500_{\varphi} - Z500_{\varphi-d\varphi}}{d\varphi} > 0 \ \frac{m}{^\circ lat} \quad (2)$$

Here, φ denotes latitude and varies from 35° to 75°. $d\varphi$ denotes how far poleward or equatorward the second grid point is located to calculate the gradients. $d\varphi$ is the highest possible multiple of the input resolution that is smaller than 15°.

2) Z500*: Following Dole & Gordon (1983), we define blocks as regions with a positive Z500 anomaly (Z500*) > 200 m.

3) VAPV: Similar to Schwierz et al. (2004), blocks are derived from the 150–500 hPa vertically averaged PV (VAPV). Blocks are detected as regions with VAPV anomalies < -1.3 (> 1.3) PVU in the Northern (Southern) hemisphere after a 2-day running mean filter is applied.

For Z500* and VAPV the anomalies are subtracted from the 30-day running mean climatology between 1979 and 2017. In all three blocking algorithms, we consider only blocks that are quasi-stationary (i.e. $A_t \geq 0.7 * A_{t+1}$, where A_t denotes the area of a block at time step t) and long-lasting (≥ 5 days).

To detect and track cyclones we use two algorithms:

1) WS06: Wernli & Schwierz (2006) detect cyclones as areas of the largest enclosed SLP contour around a SLP minima. We discard cyclones over elevated terrain (surface pressure <850 hPa) and shorter than one day. The locations of cyclogenesis and cyclolysis must be at least 1000 km apart, and we merge cyclone centers that are closer than 1000 km. For further details and refinements about the algorithm refer to Sprenger et al. (2017).
2) B97: Blender et al. (1997) define cyclones as minima at the 1000 hPa geopotential height level (Z1000). Minima are ignored if they are over elevated terrain (>1000 m) or if more than 50% of the grid points in an area within the estimated cyclone radius around the center are over elevated terrain. Only cyclones with a mean horizontal gradient of at least 30 m / 1000 km are detected. Cyclones require a minimum distance of 1000 km and a minimum duration of one day to be retained in the catalog (Raible et al., 2018).

The TM2D, Z500*, VAPV and WS06 algorithms extract binary cyclone or blocking fields. We use the Jaccard index, *J* (Jaccard, 1908), to investigate how similar ERA5 and ERA-interim are. *J* is the overlap area divided by the union area of a given feature in two reanalyses A and B during time step t: $J(t) = \frac{A(t) \cap B(t)}{A(t) \cup B(t)}$. Time steps with no blocks are set to *J(t)* = 1. Aggregated over time, we can infer the similarity between two datasets. We use this index for a crude comparison of the similarity between ERA5 and ERA-interim with two other reanalyses, CFSR (Saha et al., 2010) and MERRA-2 (Gelaro et al., 2017).

We filter the Z500 field to obtain Eulerian perspective of blocks and cyclones. Following Blackmon (1976), we retain time scales between 2.5–6 days for cyclones (Z500bp), while for blocks frequencies between 10-90 days are retained (Z500lp).

3 Results

3.1 Blocking characteristics

We compare annual blocking frequencies (denoted as the number of blocked time steps divided by the total number of time steps per grid point; Figure 1). Across all reanalysis and resolutions three blocking maxima in the North Atlantic, the North Pacific, and the South Pacific emerge as robust features. Relative blocking frequencies vary depending on the algorithm. VAPV (Figure 1i-l) and TM2D (Figure 1a-d) detect fewer blocks in the Southern Hemisphere compared to Z500* (Figure 1e-h). In the Northern Hemisphere TM2D detects more blocks in low latitudes, which are rather an imprint of the subtropical high-pressure belt (Treidl et al., 1981). This is particularly evident during summer (JJA; Supplemental Figure 1). Additionally, TM2D shows a summer peak over Siberia which is shifted north-east in VAPV and is not captured in Z500*. Overall blocking activity in winter (DJF) is generally higher than in summer (Supplemental Figure 1 and 2). The Eulerian method for blocks, Z500lp (Figure 1m-p), shows a similar distribution in the mid-latitudes as Z500* and VAPV with maxima along the Southern Hemispheric mid-latitude, over the Aleutians and over the British Islands. Blocks tend to last longer in Z500* compared to VAPV and TM2D (Figure 2a,d,g). This is also evident from the mean blocking duration of 10.2 days in Z500* compared to roughly 8.5 days in VAPV and TM2D. The mean area of a block in Z500* is largest (~ $5*10^6$ km^2) compared to TM2D (~$3.5*10^6$ km^2) and VAPV (~$3*10^6$ km^2; Figure 2b,e,h). Note that all these measures (blocking frequency, duration, and area) depend on the subjective choices of thresholds for each block algorithm.

ERA-interim and ERA5 show very similar climatological annual blocking frequencies at a 2° resolution (Figure 1b,f,j,n). Only exception is the higher (lower) lowpass-filtered Z500 variability in the Southern Ocean (Antarctica; Figure 1n). Relative differences are small (<3%) for the main blocking areas. The same holds true for other characteristics of blocks (<3%) when comparing ERA5 with ERA-interim (Figure 2; Table 1).

Block detection algorithms are also insensitive to the input resolution of ERA5 (Figure 1). The only notable difference is between 2° and 1° resolution for TM2D (Figure 1c). The increase is related to the blocking definition, which limits the latitudinal extent of a block to the biggest possible multiple of the input resolution that is no larger than 15°. Hence, we obtain a maximum latitudinal extent of 14° for a 2° resolution and a maximum of 15° for 1° resolution, i.e. a block at 1° resolution is potentially ~7% (15°/14°) larger than at 2° resolution. This also affects other blocking characteristics such as the mean duration that increases from 8.3 to 8.7 days from original to 1° and 2° resolution. Other than that, block duration (Figure 2a,d,g), block area (Figure 2b,e,h) and block intensity (Figure 2c,f,i) show no substantial differences between different input resolutions. Differences are only visible in the extreme tails of the distributions with very few blocks (note the logarithmic scale). The overall number of blocks and the number of blocking time steps for the Lagrangian methods

increases with increasing resolution (Table 1). This is expected as genesis (lysis) of blocking events tend to be detected earlier (later) with higher resolutions. The outcome of the Eulerian method Z500lp is insensitive to the input resolution.

In summary, differences between ERA-interim and ERA5 at the same resolution are comparable or smaller than the differences between different resolutions for the same reanalysis. Relating these differences to the inter-annual variability of blocks reveals that inter-annual variability is orders of magnitude larger than the differences found here (not shown).

3.2 Cyclone characteristics

All algorithms identify the storm tracks over the North Atlantic, North Pacific and a band of high cyclone frequency around the Southern Ocean (Figure 1q-ab), but local differences can be large. The Eulerian measure for cyclones, Z500bp (Figure 1q-t), shows a similar location of high cyclone activity as WS06 and B97 (Figure 1u-ab). Note again, that the absolute values of cyclone frequency cannot be directly compared due to the different definitions used.

Comparing the two reanalyses (in T63 resolution) shows that all methods (WS06, B97 and Z500bp) identify a similar spatial cyclone frequency climatology (Figure 1r,v,z). Correspondingly, the number of cyclones is relatively similar in ERA5 and ERA-interim for the T63 resolution (Table 1). We find 4% more (8% fewer) cyclones for WS06 (B97) in ERA5 compared to ERA-interim for the T63 resolution. If we only consider deep cyclones (SLP minimum < 960 hPa for WS06; Z1000 minimum < 400 m for B97 at least once in their lifetime), we find 2% (3%) more cyclones using WS06 (B97) in ERA5 than ERA-interim.

WS06 and, to an even greater extent, B97 are sensitive to changes in input resolution, whereas Z500bp is insensitive (Figure 1s,t,w,x,aa,ab). Seasonality for WS06 and Z500bp shows a peak of cyclone activity in the winter hemisphere (Supplemental Figure 1 and 2). B97 shows a peak in summer in many regions, partially related to its high sensitivity to detect heat lows (e.g. over the Sahara).

For WS06, we find a decrease of cyclone frequency by approximately 10% with increasing input resolution (Figure 1w,x) while the number of cyclones (and cyclone time steps) increases from T63 to 1° resolution by 10% and then decreases by 5% for the original resolution of ERA5 (Table 1). The latter contrasts with ERA-interim showing a steady increase. The ERA-interim behavior is expected as with higher resolution weaker cyclone can exceed threshold of the WS06 method and genesis (lysis) of cyclones can be detected earlier (later; Blender and Schubert, 2000). The ERA5 behavior is unexpected for the number of cyclones and the cyclone time steps (i.e. the sum of time steps of all cyclones). One reason lies in the merging of cyclone centers as one can see an increase in cyclone time steps from T63 to the original resolution for the non-filtered case (only topography is accounted for, but no constraint on travel distance or duration) but a decrease after filtering (Table 1). Another factor is the changed topography in the different resolutions as mountains are better represented with increasing horizontal resolution. We find that cyclone frequency decreases from T63 to 1° resolution whereas cyclone time steps increase. The reason lies in the definition of cyclone frequency per grid point without any normalization to a unit area, i.e. the area of a grid point is reduced stronger than the cyclone time steps increase. The other cyclone characteristics show that WS06 cyclones tend to be shorter with increasing input resolution (3.5 days for T63 resolution, 3.2 days for original resolution; Figure 2). The mean cyclone trajectory length also decreases from 3022 km to 2858 km from a T63 to original resolution in ERA5. Cyclone depth expressed as the minimum SLP of a cyclone is indifferent to both the choice of the reanalysis and the choice of resolution.

B97 shows a different dependence on input resolution. For ERA5 the cyclone frequency decreases between T63 and 1° resolution particularly in the Northern Hemisphere

(Figure 1z vs 1aa). Further increasing the resolution to the original resolution of ERA5 increases cyclone frequency again (Figure 1aa,ab): it is roughly 8% higher than for T63 resolution. The cyclone frequency is particularly enhanced close to high topography for the original resolution of ERA5 (e.g. on the leeside of the Andes, Figure 1ab). In contrast to WS06, the number of cyclones and the cyclone time steps steadily increase with resolution for both reanalyses (Table 1). For ERA5, we find a doubling of detected cyclones between T63 and original input resolution. Again, the reduced cyclone frequency from T63 to 1° resolution is unexpected given an increase in the number of time steps. The reason is the definition of the cyclone frequency without normalizing it to a unit area. This effect is however overcompensated be the strong increase in the time steps of cyclones when comparing the resolution 1° and the original resolution of ERA5 explaining thus the increase of cyclone frequency. Cyclone duration and distance are sensitive to the input resolution for both reanalyses (Figure 2m,o). B97 cyclones are on average shorter (from 3.4 days at T63 to 2.4 days at original resolution) and travel shorter distances (from 3753 km in T63 to 2550 km at 1° to 2404 km in original resolution).

Cyclone depth expressed as minimum Z1000 is indifferent to the choice of resolution (Figure 2n). ERA5 shows more extremely deep cyclones compared to ERA-int. The differences found between reanalyses and between different input resolutions are larger than the inter-annual variations of global cyclone counts.

3.3 Similarity between different reanalysis products

Figure 3 shows the 180-day running mean Jaccard index for all algorithms that detect features based on binary fields (TM2D, Z500*, VAPV and WS06) for 2° or T63 resolution. A linear regression finds a significantly increasing trend of the annually averaged Jaccard index for all algorithms between 1979 and 2017 at a significance level of 0.05, i.e., the differences between the reanalysis data sets become smaller. For VAPV and WS06 the Jaccard index is 0.03–0.05 lower during summer compared to other seasons. Blocks show a larger overlap than WS06, with Z500* showing a higher Jaccard index than the other two blocking algorithms, probably partially related to the average spatial extend of the detected feature in the different algorithms.

Averaged over time, we find lower values between ERA5 and CFSR or MERRA-2 than between ERA5 and ERA-interim. For example, the Jaccard index for TM2D (WS06) drops from 0.79 (0.61) between ERA5 and ERA-interim to 0.73-0.74 (0.55-0.56) for any combination of ERA5, ERA-interim, CFSR and MERRA-2 (not shown).

4 Discussion and conclusion

Different Lagrangian and Eulerian algorithms to detect blocks and cyclones are applied to the ERA5 reanalysis and compared to ERA-interim. Further, the sensitivity of cyclone and block characteristics to the spatial resolution is investigated.

Overall, blocking characteristics in ERA5 and ERA-interim are very similar (< 3% difference) and results are insensitive to the resolution with the exception of the TM2D algorithm. Depending on the employed algorithm block characteristics such as frequency, duration or average area vary substantially.

For cyclones, the dependence on the employed reanalysis is much higher than for blocks, and this dependence increases with higher resolution. Moreover, different algorithms show different dependencies. The Eulerian method using bandpass filtered geopotential height at 500 hPa is insensitive to the reanalysis and resolution. The different sensitivity of cyclone frequency for the Lagrangian methods, WS06 and B97, to resolution changes is

explained by the specific definition of cyclone frequency. Additionally, cyclones become shorter-lived with increasing resolution.

A striking difference between the WS06 and B97 methods is the sensitivity of the number of cyclones (or time steps) to the input resolution. B97 identifies more cyclones with increasing resolution in line with Blender and Schubert (2000) and Wang et al. (2016) who also found that higher spatial resolutions lead to higher cyclone counts. This is expected as weaker cyclones and early and late states within a cyclone lifetime are better represented so that thresholds of the method are exceeded more often. In contrast, the number of cyclones detected with WS06 decreases when increasing the resolution from 1° to the original resolution of ERA5. Reason for this behavior is the employed merging of cyclone centers in WS06. Thus, the merging in WS06 leads to a more consistent behavior between resolutions and reanalysis datasets, but it does so at the expense of losing secondary cyclogenesis, an important process for extreme cyclones (e.g., Ludwig et al., 2015). B97, on the other hand, shows a dramatic increase in the number of cyclones for the original resolution of ERA5 (factor of 2 compared to T63 resolution). We find a general increase in the detected number of cyclones accompanied with the detection of weak heat lows and potentially artificial lows around major mountain ridges. This goes along with the strongly decrease cyclone duration and distance with increasing resolution in B97. Indeed, Blender et al. (1997) recommended adjusting thresholds when using a data set with a different resolution than the one used to develop the method. Many cyclone detection algorithms were developed when resolutions around 1-2° were the state of the art, and they need to be adapted to added detail (and noise) that modern high-resolution datasets provide (e.g. Blender et al., 1997; Hodges, 1995; Murray & Simmonds, 1991, Wernli and Schwierz, 2006).

Based on these results, we recommend remapping datasets to a common resolution before any comparison. This is also important in the context of climate model evaluations that often rely on reanalyses as validation datasets. Moreover, users of Lagrangian methods should be cautious as sensitivity of some methods to resolution requires adjustments of the scheme (B97), and some processes are ignored by a method, e.g. secondary cyclogenesis for WS06. We have shown that comparing reanalyses and/or model data at a common resolution of T63 or even lower may be beneficial to avoid problems that can arise at higher resolutions.

We find blocks are more consistently represented than cyclones in ERA5 and ERA-interim due to their large-scale, quasi-stationary nature. ERA5 and ERA-interim are more similar recently for all examined algorithms, indicating that ERA5 and ERA-interim are less certain going back in time. Moreover, ERA5 and ERA-interim are more similar (i.e. the time averaged Jaccard index is higher) compared to CFSR or MERRA-2, arguably related to their similar reanalysis setup. Still, due to the numerous updates in ERA5 the two ECMWF reanalyses do not match. This was already shown in Rohrer et al. (2018) using a larger variety of reanalyses and several other studies confirm these findings (e.g. Tilinina et al., 2013); Wang et al., 2016, Rohrer et al., 2019). Other intercomparison studies showed that other variables, especially smaller scale and parameterized variables depend more strongly on the chosen reanalysis (e.g. Horton and Brönnimann, 2018; Sun et al., 2018).

In conclusion, block characteristics in ERA5 are similar to ERA-interim. For extra-tropical cyclones larger differences are discernible, particularly at higher horizontal input resolution and depending on the cyclone detection algorithm employed. Using the Jaccard index we find that agreement back to 1979 slightly but significantly decreases. We recommend that modeling and reanalysis intercomparison studies remap to a common, if feasible preferentially rather low resolution before applying algorithms to detect and track blocks and cyclones.

Acknowledgements

This study was supported by the Swiss National Science Foundation under Grant 143219. We acknowledge ECMWF and Copernicus Climate Change Service information for ERA5 and ERA-interim data. We thank Michael Sprenger and Heini Wernli for providing the Wernli and Schwierz (2006) cyclone tracking algorithm and their valuable comments. Data is available here: https:/boris.unibe.ch/133829/

References

Bengtsson, L., Hagemann, S., & Hodges, K. I. (2004). Can climate trends be calculated from reanalysis data? Journal of Geophysical Research D: Atmospheres, 109, 1–8. http://doi.org/10.1029/2004JD004536

Black, E., Blackburn, M., Harrison, G., Hoskins, B., & Methven, J. (2004). Factors contributing to the summer 2003 European heatwave. Weather, 59, 217–223. http://doi.org/10.1256/wea.74.04

Blackmon, M. L. (1976). A climatological spectral study of the 500 mb geopotential height of the Northern Hemisphere. Journal of the Atmospheric Sciences, 33, 1607–1623.

Blender, R., Fraedrich, K., & Lunkeit, F. (1997). Identification of cyclone-track regimes in the North Atlantic. Quarterly Journal of the Royal Meteorological Society, 123, 727–741. http://doi.org/10.1002/qj.49712353910

Blender, R., & Schubert M. (2000). Cyclone tracking in different spatial and temporal resolutions. Monthly Weather Review, 128, 377-384.

Buehler, T., Raible, C. C., & Stocker, T. F. (2011). The relationship of winter season North Atlantic blocking frequencies to extreme cold or dry spells in the ERA-40. Tellus A, 63, 212–222. http://doi.org/10.1111/j.1600-0870.2010.00492.x

Catto, J. L. (2016). Extratropical cyclone classification and its use. Reviews of Geosphysics, 54, 486–520. http://doi.org/10.1002/2016RG000519

Dee, D. P., Uppala, S. M., Simmons, A. J., Berrisford, P., Poli, P., Kobayashi, S., et al. (2011). The ERA-Interim reanalysis: configuration and performance of the data assimilation system. Quarterly Journal of the Royal Meteorological Society, 137, 553–597. http://doi.org/10.1002/qj.828

Dole, R. M. & Gordon, N. D. (1983). Persistent anomalies of the extratropical Northern Hemisphere wintertime circulation structure. Monthly Weather Review, 114, 178–207. http://doi.org/10.1175/1520-0493(1986)114<0178:PAOTEN>2.0.CO;2

Gelaro, R., McCarty, W., Suárez, M. J., Todling, R., Molod, A., Takacs, L., et al. (2017). The Modern-Era Retrospective Analysis for Research and Applications, Version 2 (MERRA-2). Journal of Climate, 30, 5419–5454. http://doi.org/10.1175/JCLI-D-16-0758.1

Hersbach, H., & Dee, D. P. (2016). ERA5 reanalysis is in production. ECMWF Newsletter, Number 147, 7.

Hodges, K. I. (1995). Feature tracking on the unit sphere. Monthly Weather Review, 123, 3458-3465.

Horton, P., & Brönnimann, S. (2018). Impact of global atmospheric reanalyses on statistical precipitation downscaling. Climate Dynamics, 52, 5189 – 5211. http://doi.org/10.1007/s00382-018-4442-6

Jaccard, P. (1908). Nouvelles recherches sur la distribution florale. Bulletin de la Société Vaudoise des Sciences Naturelles, 44, 223–270.

Lau, W. K. M., & Kim, K.-M. (2012). The 2010 Pakistan flood and Russian heat wave: Teleconnection of hydrometeorological extremes. Journal of Hydrometeorology, 13, 392–403. http://doi.org/10.1175/JHM-D-11-016.1

Lenggenhager, S., & Martius, O. (2019). Atmospheric blocks modulate the odds of heavy precipitation events in Europe. Climate Dynamics. https://doi.org/10.1007/s00382-019-04779-0

Ludwig, P., Pinto, J. G., Hoepp, S. A., Fink, A. H. and Gray, S. L. (2015). Secondary cyclogenesis along an occluded front leading to damaging wind gusts: Windstorm Kyrill, January 2007. Monthly Weather Review, 143, 1417-1437.

Martius, O., Sodemann, H., Joos, H., Pfahl, S., Winschall, A., Croci-Maspoli, M., et al. (2013). The role of upper-level dynamics and surface processes for the Pakistan flood of July 2010. Quarterly Journal of the Royal Meteorological Society, 139, 1780–1797. http://doi.org/10.1002/qj.2082

Messmer, M., Gómez-Navarro, J. J., & Raible, C. C. (2015). Climatology of Vb cyclones, physical mechanisms and their impact on extreme precipitation over Central Europe. Earth System Dynamics, 6, 541–553. http://doi.org/10.5194/esd-6-541-2015

Murray, R. J., & Simmonds I. (1991). A numerical scheme for tracking cyclone centers from digital data. Part I: Development and operation of the scheme. Australian Meteorlogical Magazine, 39, 155-166.

Neu, U., Akperov, M. G., Bellenbaum, N., Benestad, R., Blender, R., Caballero, R., et al. (2013). IMILAST: A community effort to intercompare extratropical cyclone detection and tracking algorithms. Bulletin of the American Meteorological Society, 94, 529–547. http://doi.org/10.1175/BAMS-D-11-00154.1

Pfahl, S., & Wernli, H. (2012). Quantifying the relevance of cyclones for precipitation extremes. Journal of Climate, 25, 6770–6780. http://doi.org/10.1175/JCLI-D-11-00705.1

Rohrer, M., Brönnimann, S., Martius, O., Raible, C. C., Wild, M., & Compo, G. P. (2018). Representation of extratropical cyclones, blocking anticyclones, and alpine circulation types in multiple reanalyses and model simulations. Journal of Climate, 31, 3009–3031. http://doi.org/10.1175/JCLI-D-17-0350.1

Rohrer, M., Brönnimann, S., Martius, O., Raible, C. C., & Wild, M. (2019). Decadal variations of blocking and storm tracks in centennial reanalyses. Tellus A, 71, 1-21. https://doi.org/10.1080/16000870.2019.1586236

Raible, C. C., Della-Marta, P., Schwierz, C., Wernli, H., & Blender, R. (2008). Northern Hemisphere extratropical cyclones: A comparison of detection and tracking methods and different reanalyses, Monthly Weather Review, 136, 880-897.

Raible, C. C., Messmer, M., Lehner, F., Stocker, T. F., & Blender, R. (2018). Extratropical cyclone statistics during the last millennium and the 21st century. Climate of the Past, 14, 1499-1514.

Saha, S., Moorthi, S., Pan, H.-L., Wu, X., Wang, J., Nadiga, S., et al. (2010). The NCEP climate forecast system reanalysis. Bulletin of the American Meteorological Society, 91, 1015–1057. http://doi.org/10.1175/2010BAMS3001.1

Scherrer, S. C., Croci-Maspoli, M., Schwierz, C., & Appenzeller, C. (2006). Two-dimensional indices of atmospheric blocking and their statistical relationship with winter climate patterns in the Euro-Atlantic region. International Journal of Climatology, 26, 233–249. http://doi.org/10.1002/joc.1250

Schwierz, C., Croci-Maspoli, M., & Davies, H. C. (2004). Perspicacious indicators of atmospheric blocking. Geophysical Research Letters, 31, L06125. http://doi.org/10.1029/2003GL019341

Shaw, T. A., Baldwin, M., Barnes, E. A., Caballero, R., Garfinkel, C. I., Hwang, Y.-T., et al. (2016). Storm track processes and the opposing influences of climate change. Nature Geoscience, 9, 656–664. http://doi.org/10.1038/ngeo2783

Sprenger, M., Fragkoulidis, G., Binder, H., Croci-Maspoli, M., Graf, P., Grams, C. M., et al. (2017). Global climatologies of Eulerian and Lagrangian flow features based on

ERA-Interim. Bulletin of the American Meteorological Society, 98, 1739–1748. http://doi.org/10.1175/BAMS-D-15-00299.1

Sun, Q., Miao, C., Duan, Q., Ashouri, H., Sorooshian, S., & Hsu, K.-L. (2018). A review of global precipitation data sets: Data sources, estimation, and intercomparisons. Reviews of Geophysics, 56, 79–107. http://doi.org/10.1002/2017RG000574

Tibaldi, S., & Molteni, F. (1990). On the operational predictability of blocking. Tellus A, 42, 343–365. http://doi.org/10.1034/j.1600-0870.1990.t01-2-00003.x

Tilinina, N., Gulev, S. K., Rudeva, I., Koltermann, P., Tilinina, N., Gulev, S. K., et al. (2013). Comparing cyclone life cycle characteristics and their interannual variability in different reanalyses. Journal of Climate, 26, 6419–6438. http://doi.org/10.1175/JCLI-D-12-00777.1

Treidl, R. A., Birch, E. C., & Sajecki, P. (1981). Blocking action in the Northern Hemisphere: A climatological study. Atmosphere-Ocean, 19, 1–23. https://doi.org/10.1080/07055900.1981.9649096

Wang, X. L., Feng, Y., Chan, R., & Isaac, V. (2016). Inter-comparison of extra-tropical cyclone activity in nine reanalysis datasets. Atmospheric Research, 181, 133–153. http://doi.org/10.1016/j.atmosres.2016.06.010

Wernli, H., & Schwierz, C. (2006). Surface cyclones in the ERA-40 dataset (1958–2001). Part I: Novel identification method and global climatology. Journal of Atmospheric Sciences, 63, 2486–2507.

Woollings, T., Barriopedro, D., Methven, J., Son, S.-W., Martius, O., Harvey, B., et al. (2018). Blocking and its response to climate change. Current Climate Change Reports, 4, 287–300. http://doi.org/10.1007/s40641-018-0108-z

Table 1: Number of blocks and cyclones detected globally in ERA5 and ERA-interim between 2000 and 2017 using different blocking (upper part) and cyclone (lower part) algorithms and resolutions. WS06deep presents results for deep cyclones only (i.e. cyclones with a SLP minimum < 960 hPa respectively. For B97deep <-400m). Also the number of block or cyclone time steps per algorithm is given. For WS06 additionally the number of cyclone time steps before any filtering is given.

Algorithm		*ERA5*			*ERA-interim*		
Resolution	**Type**	**Orig**	**1°**	**2°**	**Orig**	**1°**	**2°**
VAPV	Blocks	4585	4528	4310	-	4412	4234
TM2D	Blocks	3563	3502	3437	3631	3488	3389
Z500*	Blocks	2491	2482	2465	2495	2489	2462
VAPV	Timesteps	156 702	154 631	146 735	-	149 950	142 816
TM2D	Timesteps	124 747	122 460	114 768	126 863	121 461	112 887
Z500*	Timesteps	101 754	101 229	99 635	102 366	101 761	100 131
Resolution		**Orig**	**1°**	**T63**	**Orig**	**1°**	**T63**
WS06	Cyclones	83 656	88 334	80 059	86 195	85 183	76 701
WS06deep	Cyclones	13 726	14 088	12 637	14 030	13 725	12 361
B97	Cyclones	198 440	150 691	94 554	135 854	127 706	102 357
B97deep	Cyclones	4148	3655	2199	3176	2894	2134
WS06	Timesteps	1 073 444	1 170 977	1 132 062	1 203 202	1 201 374	1 096 298
WS06 (no filter)	Timesteps	2 487 269	2 565 175	2 339 972	2 392 562	2 356 335	2 209 104
B97	Timesteps	2 129 026	1 741 991	1 507 054	1 678 702	1 588 450	1 450 087

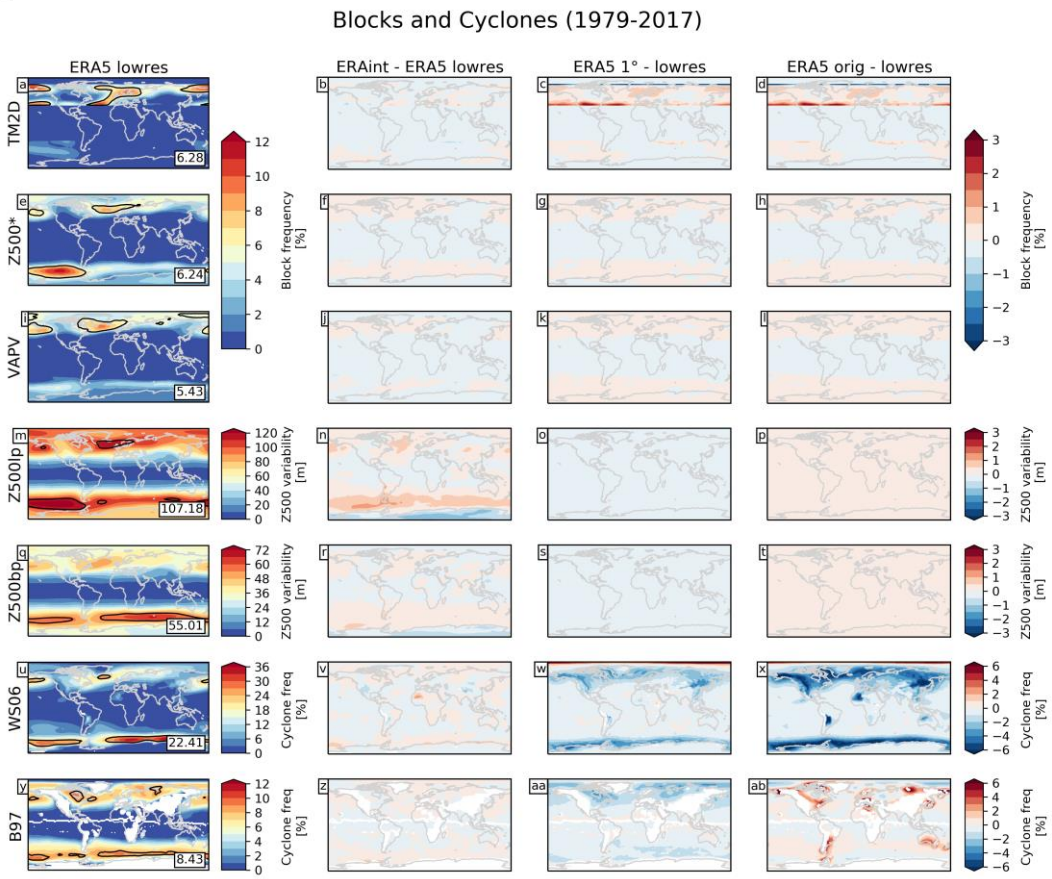

Figure 1: Climatological distribution (1979 – 2017) of blocks and cyclones in ERA5 remapped to low resolution (left column) and the difference to ERA-interim (second column), ERA5 at a 1° resolution (third column) and ERA5 at original resolution (last column). The upper four rows show the different block algorithms (TM2D, Z500*, VAPV and Z500lp). The lower three rows show the cyclone distributions determined by Z500bp, WS06 and B97. For WS06 we show the cyclone frequency defined as cyclone presence at a grid point using the outer contour as area. For B97 the cyclone frequency is defined as cyclone presence at the grid point (without normalizing it to a unit area; Raible et al. 2018), i.e., first each grid point within the radius of a cyclone (using a two dimensional Gaussian fit to the center) is assigned to be occupied by the cyclone for on time step. Summing over all time steps for each grid point and dividing by the total number of time steps results in cyclone frequency at each grid point in %. The value of the black 95th percentile contour is given in the lower right of each panel.

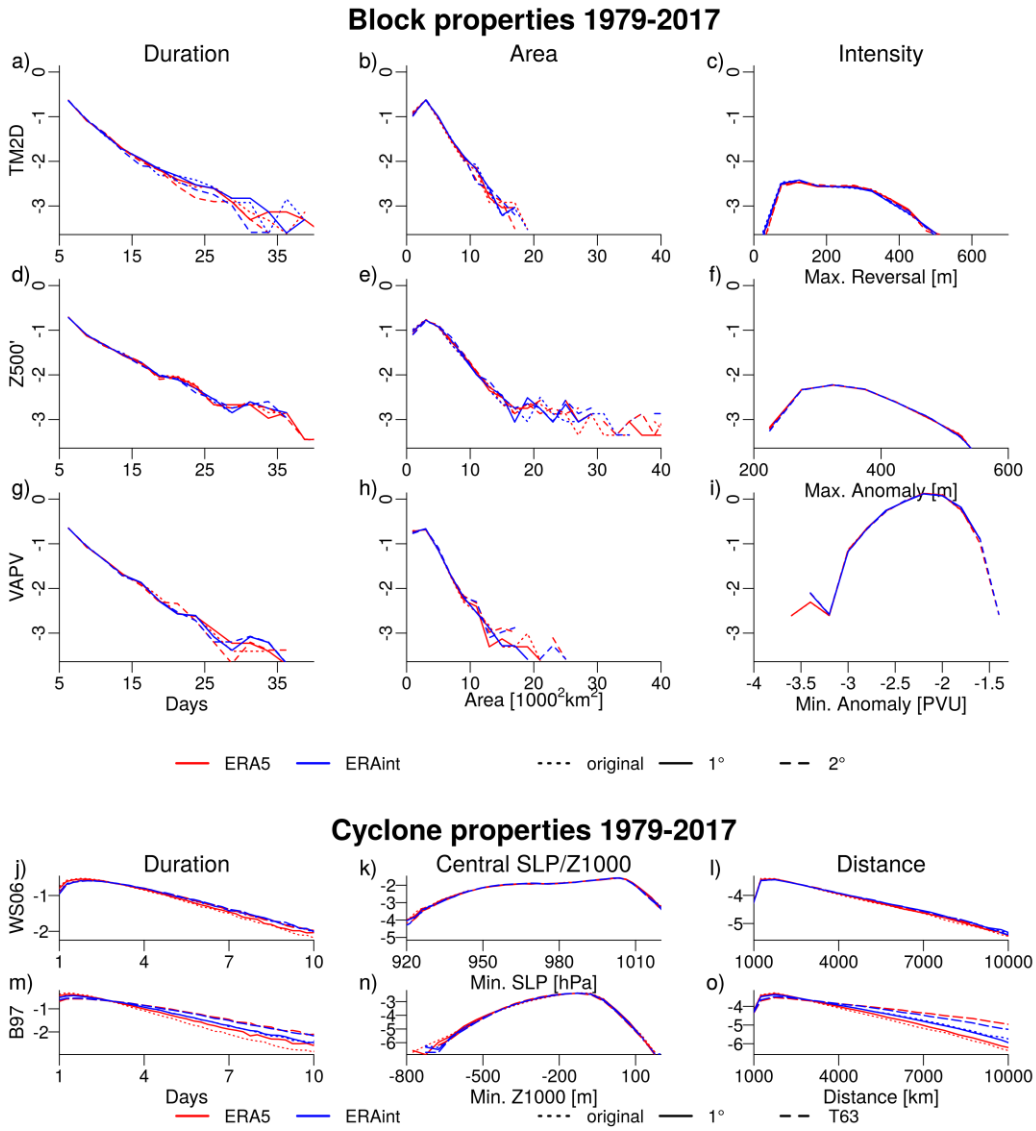

Figure 2: The probability distribution function for block duration, block area and block intensity for different blocking algorithms (upper part). The lower part shows the probability density function for cyclone duration, central pressure-geopotential height and the distance travelled between cyclone genesis to lysis. ERA5 is shown in red, ERA-interim in blue. The line type distinguishes different input resolutions. For presentational reasons the y axis only shows the exponent of the logarithmic scale (e.g. -3 denotes 10^{-3}).

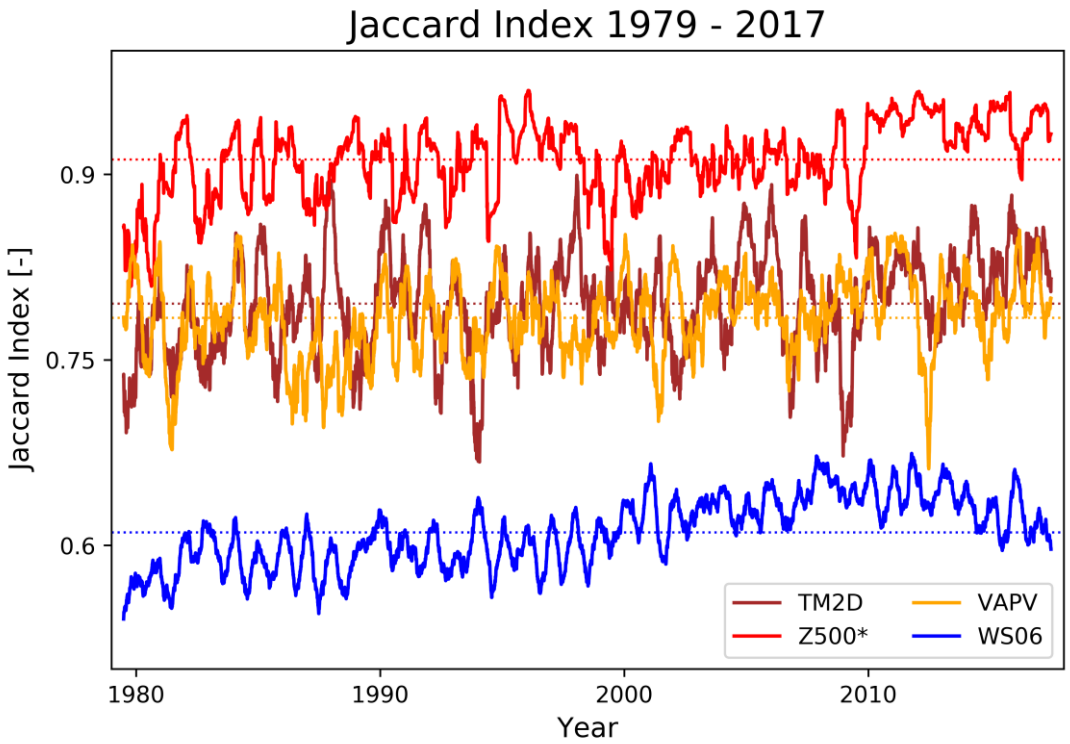

Figure 3: Jaccard Index for TM2D, Z500, VAPV and WS06 as a measure of the spatial overlap of features between ERA5 and ERA-interim over time. A 180-day running mean for better readability. The dashed line denotes time average between 1979 and 2017.